

## Acidic treatment of sodium sulfide by-product sediment to recover sodium oxide and preparation porous ceramics for building applications

Changrong Liu<sup>a</sup>, Hongbin Tan<sup>a,b,\*</sup>, Aiguo Zheng<sup>c</sup>, Xiangmei Kang<sup>c</sup>, Ao Jiang<sup>c</sup>, Rui Fang<sup>a</sup>, Haorong Ren<sup>a</sup> and Wanwei Fang<sup>d</sup>

<sup>a</sup>State Key Laboratory of Environment-friendly Energy Materials, School of Materials Science and Engineering, Southwest University of Science and Technology, Mianyang Sichuan 621010, China

<sup>b</sup>Shaanxi Engineering Center of Metallurgical Sediment Resource, Shaanxi University of Technology, Hanzhong Shaanxi 723000, China

<sup>c</sup>Deyang Rail Co., Ltd. of Chengdu Railway, Deyang Sichuan 618007, China

<sup>d</sup>Xinjiang Changji Construction Group, Changji Xinjiang 831100, China

The manufacture of sodium sulfide through a carbon reduction process, using sodium sulfate as raw material, generates sodium sulfide by-product sediment, which has potential health and environmental impacts. Herein, a novel strategy is proposed to recover sodium oxide from the sediment by using acidic treatment and the influence of solution pH on sodium oxide content is systematically studied. The results reveal that the sodium oxide content decreases with decreasing pH value of the solution. At pH = 4, the as-treated sediment results in Na<sub>2</sub>O content of 3.10 wt. %, which recovery rate is about 90%. Furthermore, the influences of sintering temperature and time on compressive strength and bulk density are studied. In general, the compressive strength and bulk density increase with increasing sintering temperature and time. After sintering at 1,300 °C for 120 min, the compressive strength and bulk density of the sintered porous ceramic are 26.66 MPa and 1.31 g/cm<sup>3</sup>, respectively. The porous ceramic, sintered at 1,300 °C, mainly consists of hauyne, gehlenite and hematite phases. In summary, the few flaws in cell-walls result in high compressive strength of the as-prepared porous ceramics.

**Key words:** sodium sulfide, alkaline sediment, acid treatment, porous ceramic, waste utilization.

### Introduction

One of the most important challenges in design of future buildings is to reduce the overall energy consumption in all their life phases, from construction to demolition [1]. The building energy consumption is mainly caused by the high heating and air conditioning energy consumption, which can be attributed to the high heat transfer coefficient of the traditional building envelop [2]. Building insulation materials, including insulative composites, offer resistance to heat flow and improve the indoor thermal environment by decreasing the heating- and cooling-load of the buildings [3].

Porous ceramics with tunable pore structure, including size, volume, connectivity and shape, are widely used as the thermal and acoustic insulators in modern buildings [4]. The inorganic ceramic materials render distinct advantages, such as stable performance, fire retardant, anti-aging and eco-friendly, which make them promising materials for building insulation [5].

For instance, sodium sulfide (Na<sub>2</sub>S) is widely used in different fields, such as dyeing, mineral separation, pigment and rubber products [6-8]. The manufacturing of Na<sub>2</sub>S is carried out by various methods, including carbon reduction, hydrogen sulfide, barium sulfide and gas reduction method. Carbon reduction is still a preferred method to synthesis Na<sub>2</sub>S due to its simplicity and cost-effectiveness. In carbon reduction method, sodium sulfate is reduced with coal at high temperature to obtain black-colored sodium sulfide, which renders further Na<sub>2</sub>S products through subsequent leaching, washing and evaporation steps. However, the as-received sediment (sodium sulfide by-product, 3SP) contains, Na<sub>2</sub>O, SO<sub>3</sub>, CaO, SiO<sub>2</sub>, Al<sub>2</sub>O<sub>3</sub> and other impurity. In addition, the strongly alkaline sediment is dumped in large stockpiles, which are exposed to the weathering process and exhibit potential health and environmental hazards. Therefore, the effective reutilization of the sediment is highly desirable from environmental and economic viewpoints.

In generally, zeolite is easy to form when fly ash is treated in NaOH aqueous solution. The Na<sup>+</sup> in zeolite can be substituted by H<sup>+</sup> or other cations. As a result, Na<sub>2</sub>O would be retrieved by sulphuric acid treatment. In particular, it is of utmost importance to retrieve

\*Corresponding author:  
Tel : +86 816 2419201  
Fax: +86 816 2419201  
E-mail: hb-t@163.com

sodium oxide ( $\text{Na}_2\text{O}$ ) and reutilize the sediment to obtain lightweight building materials.

With the increasing demand for building materials, natural resources are reaching critical and distressing levels. Moreover, increased solid-waste and environmental concerns have triggered widespread interest in recycling of waste materials for a variety of applications. Hence, the utilization of solid-waste, as a replacement of raw building materials, is desired to protect natural resources and relieve pressure of the increasing solid-waste [9].

One should note that the porous ceramics are prepared from a variety of solid-waste, such as fly ash, waste-glass, germanium tailings, etc. For instance, Wang et al. [10] have obtained insulation ceramic tiles by using fly ash, waste-glass and clay. Similarly, Zhang et al. [11] have synthesized glass ceramic foams by using cathode ray tube, germanium tailings, sodium borate and  $\text{NaNO}_3$  as raw materials. Despite these preliminary studies on utilization of solid-waste into building materials, the recycling of sodium sulfide by-product sediment (3SP) has been rarely carried out to fabricate porous ceramics. On the other hand, these processes are complex and utilize multiple raw materials, resulting in increased product cost.

Herein, we aim to retrieve sodium oxide from 3SP by sulphuric acid treatment and only reutilize the acidulated 3SP raw material to obtain porous ceramic materials for building applications. Moreover, the influences of sintering temperature and time on compressive strength, bulk density, crystal structure and morphology of porous ceramic will be systematically studied.

## Experimental Procedure

Sulphuric acid (analytical grade, concentration 98%) was provided by Chengdu Kelong Chemical Reagent Co. Ltd., China. 3SP was provided by Sichuan Shenhong Chemical Industry Co., Ltd., China. The radioactivity of 3SP is not harmful to human health as per the Chinese national standard, “*Limits of radionuclides in building materials (GB 6566-2010)*”.

In a typical process, 3SP and tap water were added, with a mass ratio of 1:5, in a beaker. Then, sulphuric acid was added to obtain a pH value of 9, 7, 5, 4, respectively. Then, the solution was stirred and aerated at 25 °C for 3 h. Finally, the treated samples were vacuum filtered to obtain an green acidulated 3SP, which was dried at 105 °C for 24 h.

The green acidulated 3SP slurry was poured into a mold (20 × 20 × 20 mm) and shaped by externally

applied pressure. The molds were removed after 24 h of drying at 40 °C. Finally, the dried samples were loaded into a muffle furnace and sintered at various temperatures (900, 1000, 1100 and 1,200 °C) for different times (30, 30, 90 and 120 min).

The chemical composition of raw material was analyzed by an X-ray fluorescence spectrometer (XRF, Axios-Poly, PANalytical, Netherlands). The morphology was observed by scanning electron microscopy (SEM, TM-2000/4000, Hitachi, Japan). The phase analysis was carried out by using X-ray powder diffractometer (XRD, Ultima IV, Rigaku, Japan), equipped with  $\text{Cu K}\alpha$  radiations ( $\lambda = 0.15406$  nm). The compressive strength was measured by using a computer controlled micro-electromechanical universal testing machine (104C, Shenzhen Wance Testing Machine, China) at a loading rate of 0.02 kN/s. The density of the sintered sample was analyzed by the Archimedes method by using tap water as the liquid medium.

## Results and Discussion

The chemical composition and X-ray diffraction (XRD) pattern of as-received 3SP are presented in Table 1 and Fig. 1, respectively. The as-received 3SP contains 31.81 wt.%  $\text{SO}_3$ , 30.88 wt.%  $\text{Na}_2\text{O}$ , 12.47 wt.%  $\text{SiO}_2$ , 10.15 wt.%  $\text{Al}_2\text{O}_3$ , 6.69 wt.%  $\text{CaO}$  and 6.10 wt.%  $\text{Fe}_2\text{O}_3$ . The major phases in 3SP are zeolite ( $1.0\text{Na}_2\text{O}\cdot\text{Al}_2\text{O}_3\cdot 1.68\text{SiO}_2\cdot 1.73\text{H}_2\text{O}$ , PDF 31-1270), erdite ( $\text{NaFeS}_2\cdot 2\text{H}_2\text{O}$ , PDF 33-1253), calcium iron oxide ( $\text{CaFeO}_3$ , PDF 41-0753), whereas minor phases are margarite ( $\text{CaAl}_2(\text{Al}_2\text{Si}_2)\cdot 10(\text{OH})_2$ , PDF 74-1190), katoite ( $\text{Ca}_3\text{Al}_2\text{O}_6(\text{OH})_6$ , PDF 71-0735), Melanterite ( $\text{FeSO}_4\cdot 7\text{H}_2\text{O}$ , PDF 76-0657) and lisetite ( $\text{CaNa}_2\text{Al}_4\text{Si}_4\text{O}_{16}$ , PDF 76-0657).

The amount of sodium oxide in acidulated 3SP is presented in Fig. 2. It can be readily observed that the sodium oxide content decreases with decreasing pH value of the solution. The 3SP contains zeolite phase, which can adsorb  $\text{Na}^+$  ions. When the pH values is decreased, the content of other cations, such as  $\text{Ca}^{2+}$ ,  $\text{Al}^{3+}$  and  $\text{Fe}^{3+}$ , increase in the solution and, then, the  $\text{Na}^+$  in zeolite are substituted by  $\text{H}^+$  or other cations. On the other hand, 3SP is obtained from the reducing atmosphere, where the solution was aerated to oxidize  $\text{Fe}^{2+}$  into  $\text{Fe}^{3+}$  ions and inhibit the incorporation of ferrous cations into the filtrate. The chemical composition of acidulated 3SP is presented in Table 1. The 3SP contains 3.10 wt.%  $\text{Na}_2\text{O}$  after treating in a solution with pH = 4, which  $\text{Na}_2\text{O}$  recovery rate is about 90%. Under

**Table 1.** Chemical composition of sediments (wt. %).

Sediment	$\text{SO}_3$	$\text{Na}_2\text{O}$	$\text{SiO}_2$	$\text{Al}_2\text{O}_3$	$\text{CaO}$	$\text{Fe}_2\text{O}_3$	$\text{TiO}_2$	$\text{MgO}$	Others
Received	31.81	30.88	12.47	10.15	6.69	6.10	0.74	0.73	0.43
pH4	38.13	3.10	20.49	15.84	11.98	8.28	1.43	0.30	0.45

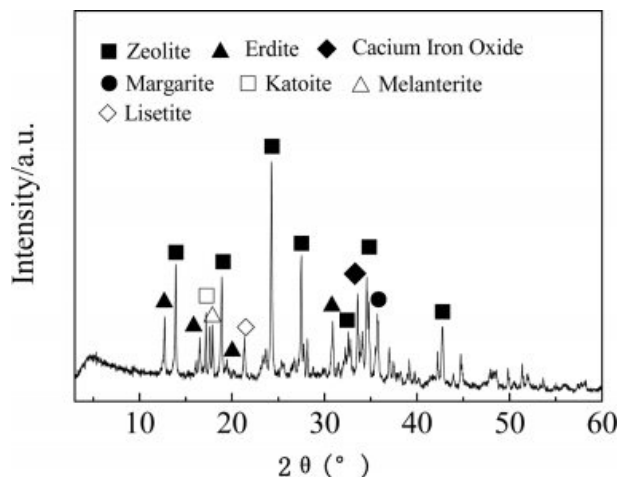


Fig. 1. XRD pattern of sodium sulfide by-product sediment.

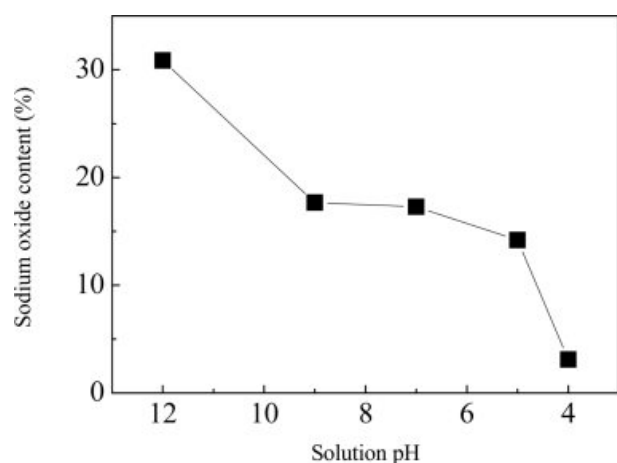


Fig. 2. Sodium oxide content of the different acidulated 3SP samples.

decreasing pH values, more cations, such as  $\text{Al}^{3+}$ ,  $\text{Fe}^{3+}$  and  $\text{Ca}^{2+}$ , incorporate into the filtrate, which implies that the optimal pH value of 4 should be used for further experiments.

The compressive strength and bulk density of the porous ceramic samples, sintered at different temperatures for 2 h, are presented in Fig. 3. It can be readily observed that the compressive strength and bulk density increase with increasing sintering temperature. In particular, the compressive strength and bulk density rapidly increase after sintering in the temperature range of 1,200 to 1,300 °C. After sintering at 1,200 °C and 1,300 °C, the compressive strength and bulk density of porous ceramic are 5.92 and 26.66 MPa, and 1.24 and 1.31 g/cm<sup>3</sup>, respectively. However, a further increase in sintering temperature (1,400 °C) results in the appearance deformation of the cubic sample. Hence, the optimal sintering temperature of 1,300 °C is used for further analysis.

The XRD patterns of the porous ceramic samples, sintered at different temperatures, are presented in Fig.

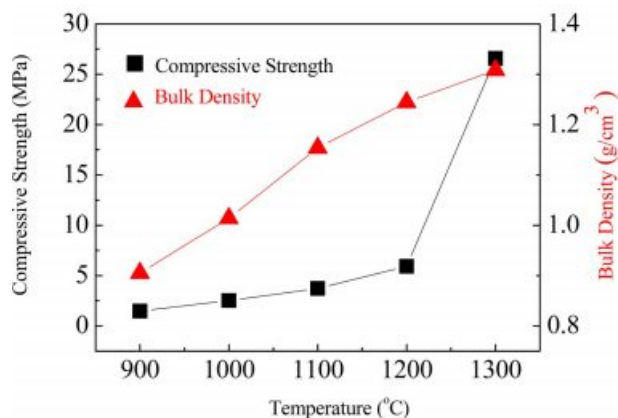


Fig. 3. Compressive strength and density of the porous ceramic samples sintered at different temperature for 2 h.

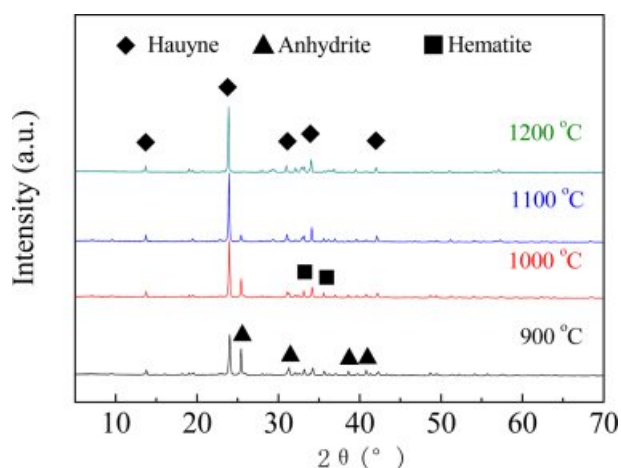
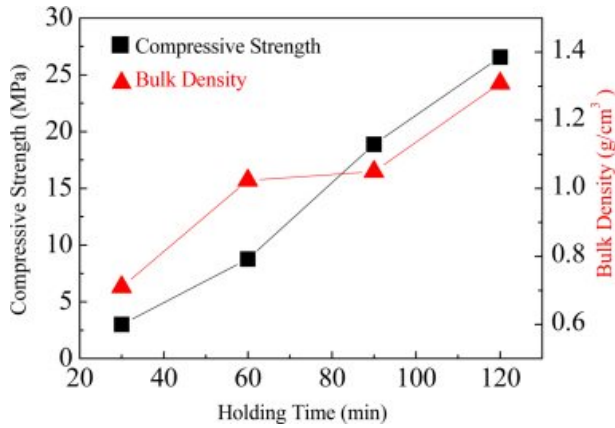


Fig. 4. XRD patterns of the porous ceramic samples sintered at different temperature for 2 h.

4. After sintering at 900 °C for 2 h, the as-prepared sample exhibits the presence of hauyne ( $\text{Na}_6\text{Ca}_2\text{Al}_6\text{Si}_6\text{O}_{24}(\text{SO}_4)_2$ , PDF#37-0473), anhydrite ( $\text{Ca}(\text{SO}_4)$ , PDF#72-0916) and hematite ( $\text{Fe}_2\text{O}_3$ , PDF#85-0599) phases. However, the diffraction peaks of anhydrite become weaker with increasing sintering temperature due to anhydrite decomposition. After sintering at 1,200 °C for 2 h, the anhydrite phase has been observed as the minor phase, whereas the hauyne and hematite phases have been observed as the major phases. One should note that the hematite diffraction peaks originate from the presence of iron-based compounds in 3SP.

However, the as-prepared sample, sintered at 1,200 °C, exhibits inferior compressive strength due to the absence of liquid phase sintering and anhydrite decomposition. However, the samples have demonstrated obvious matrix densification and volumetric shrinkage after being sintered at 1,300 °C, which can be ascribed to the liquid-phase sintering due to liquid phase formation.

The compressive strength and bulk density of the samples, sintered at 1,300 °C for different times, are



**Fig. 5.** Compressive strength and bulk density of the porous ceramic samples sintered at 1,300 °C for different time.

presented in Fig. 5. One should note that the compressive strength and bulk density exhibit a direct relationship with sintering time. At the sintering time of 90 min, the compressive strength and bulk density are 18.88 MPa and 1.051 g/cm<sup>3</sup>, respectively, which increase to 26.66 MPa and 1.31 g/cm<sup>3</sup> after being sintering at 1,300 °C for 120 min.

The XRD patterns of the porous ceramic samples, sintered at 1,300 °C for different times, are presented in Fig. 6. After sintering at 1,300 °C for 30 min, the as-

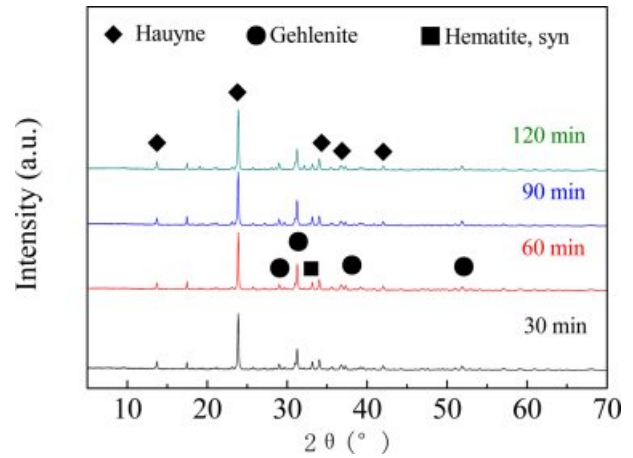


**Fig. 6.** XRD patterns of the porous ceramic samples sintered at 1,300 °C for different time.

prepared sample exhibits hauyene ( $\text{Na}_6\text{Ca}_2\text{Al}_6\text{Si}_6\text{O}_{24}(\text{SO}_4)_2$ , PDF#37-0473), gehlenite ( $\text{Ca}_2\text{Al}(\text{AlSi})\text{O}_7$ , PDF#89-5917) and hematite (syn,  $\text{Fe}_2\text{O}_3$ , PDF#89-0596) phases. However, unlike sintering at 1,200 °C, these phases do not change with sintering time.

The SEM images of the porous ceramic samples, sintered at 1,300 °C for different times, are shown in Fig. 7. It can be readily observed that the pore number decrease with increasing holding time. Initially, the pore

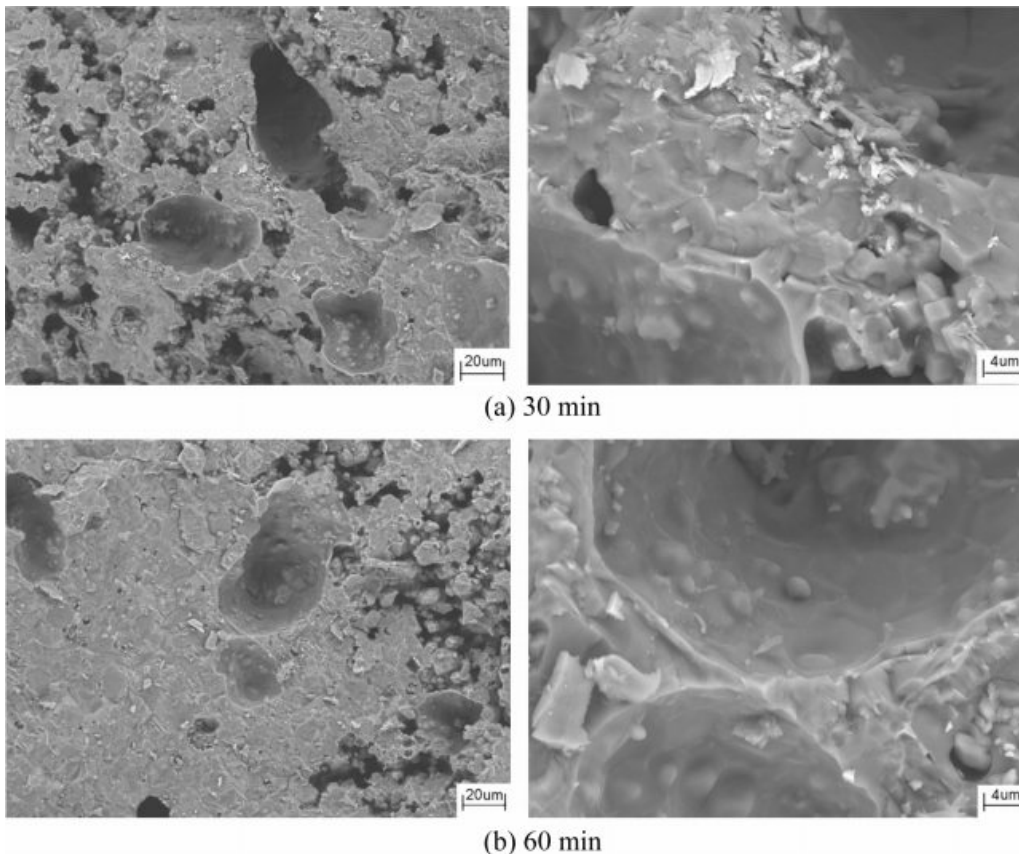


**Fig. 7.** SEM images of the porous ceramic sample sintered at 1,300 °C for different time.

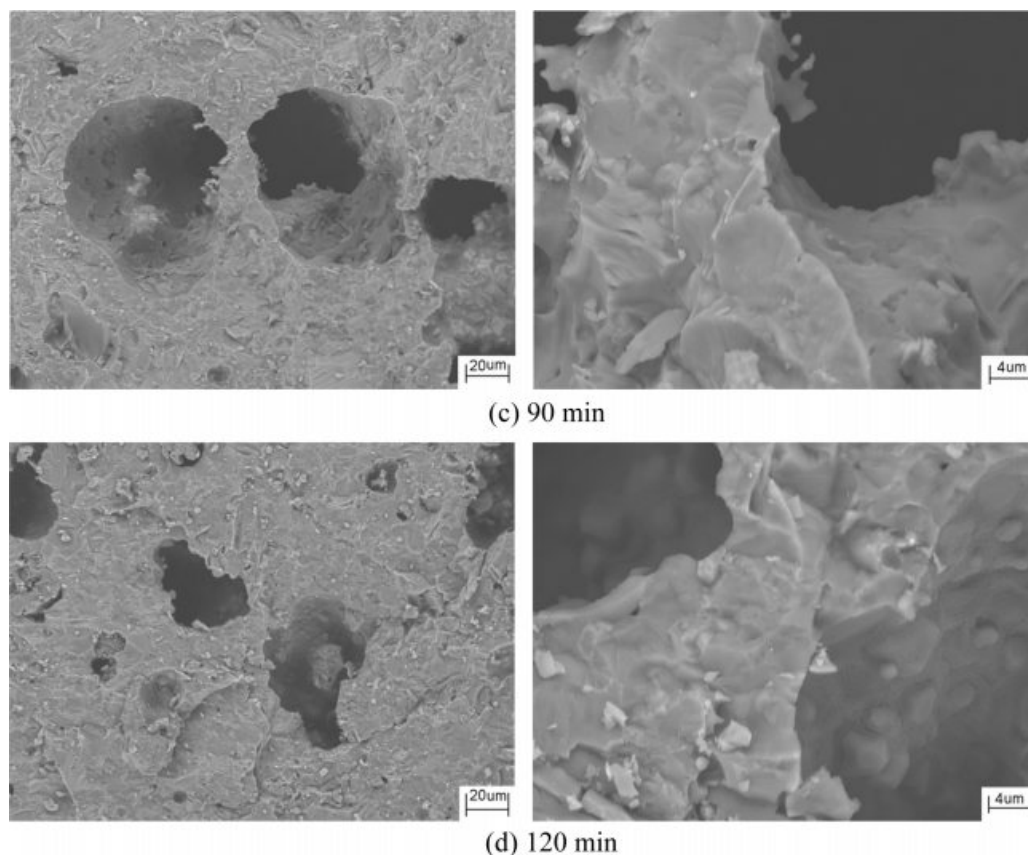


**Fig. 7.** SEM images of the porous ceramic sample sintered at 1,300 °C for different time (continued).

size increases with increasing holding time, follows by a gradual decrease. Once the holding time is increased to 90 min, the coalescence phenomenon occurred, i.e., smaller pores tend to dissolve in larger pores, to decrease the surface energy of the system. The number of tiny pores in the cell walls (struts), which limit the strength of porous ceramic, also decrease due to sintering.

It is worth mentioning that the foaming agents are usually used to prepare porous ceramics [12]. Herein, the acidulated 3SP sediment contains calcium sulfate, which decomposes at  $\sim 1,200$  °C. As a result, the as-generated  $\text{SO}_2$  gas is besieged by the softened glass phase, which acts as a foaming agent and results in a porous structure. However, the resulting pores exhibit a less uniform pore size and aspherical morphology due to insufficient liquid-phase at high temperature (1,300 °C). The type of porous structure and cell-walls determine the mechanical strength of porous ceramic. For instance, Kazantseva et al. [13] have obtained lightweight porous ceramics by alkaline activation of zeolite, which rendered high strength and low density due to the microporous structure of the zeolite. Herein, the as-receive 3SP also contains zeolite phase, which might have a positive influence on porous structure and mechanical properties. However, this is beyond the scope of current research and shall be studied in future work.

## Conclusions

The sodium oxide contents decrease with decreasing pH value of the 3SP solution, which pH value is changed by adding sulphuric acid. The acidulated 3SP exhibits 3.10 wt.%  $\text{Na}_2\text{O}$  after being treated with sulphuric solution (pH = 4), which  $\text{Na}_2\text{O}$  recovery rate is about 90%. The compressive strength and bulk density of porous ceramic sample increase with increasing sintering temperature and holding time. Moreover, the compressive strength of porous ceramic sample has exhibited a direct relationship with its bulk density. After sintering at 1,300 °C for 120 min, the compressive strength and bulk density of sample are 26.66 MPa and  $1.31 \text{ g/cm}^3$ , respectively. Moreover, the porous ceramic sample consists of haunyne, gehlenite and hematite phases. The few flaws are observed in porous ceramic cell-walls, which ceramic has high compressive strength.

## Acknowledgements

This work was supported by the Research Fund of the Sichuan Science and Technology Program of China (2019YFG0518) and Natural Science Foundation of Southwest University of Science and Technology (19zx7130).

### References

1. F. Asdrubali, F. Dalessandro, and S. Schiavoni, *Sustain. Mater. Techn.* 4[7] (2015) 1-17.
2. H. Wang, Z. Chen, R. Ji, L. Liu, and X. Wang, *Ceram. Int.* 44[12] (2018) 13681-13688.
3. X. Su, Z. Luo, Y. Li, and C. Huang, *J. Clean. Prod.* 112[1] (2016) 275-281.
4. H. Alghamdi, A. Dakhane, A. Alum, M. Abbaszadegan, B. Mobasher, and N. Neithalath, *Mater. Design.* 152 [8] (2018) 10-21.
5. L. Zhu, S. Li, Y. Li, and N. Xu, *Constr. Build. Mater.* 180[8] (2018) 291-297.
6. T. A. Nguyen and R-S. Juang, *Chem. Eng. J.* 219[3] (2013) 109-117.
7. Q. Zhao, W. Liu, D. Wei, W. Wang, B. Cui, and W. Liu, *Miner. Eng.* 115[1] (2018) 44-52.
8. N. Gobeltz, LedéB, K. Raulin, A. Demortier, and J. P. Lelieur, *Micropor. Mesopor. Mat.* 141[1-3] (2011) 214-221.
9. T. Liu, Y. Tang, L. Han, J. Song, Z. Luo, and A. Lu, *Ceram. Int.* 43[6] (2017) 4910-4918.
10. H. Wang, Y. Sun, L. Liu, X. Wang, and R. Ji, *Energ. Buildings.* 168[6] (2018) 67-75.
11. Q. Zhang, F. He, H. Shu, Y. Qiao, S. Mei, M. Jin, and J. Xie, *Constr. Build. Mater.* 111[5] (2016) 105-110.
12. M. Zhu, R. Ji, Z. Li, H. Wang, L. Liu, and Z. Zhang, *Constr. Build. Mater.* 112[6] (2016) 398-405.
13. L.K. Kazantseva and S. V. Rashchenko, *Ceram Int.* 42[16] (2016) 19259-19265.